Microstructural and deformational studies on mylonite in the detachment faults of Yalashangbo dome, North Himalayan domes zone*

ZHANG Bo**, ZHANG Jinjiang*, GUO Lei and WANG Weiliang

(Department of Geology, School of Earth and Space Sciences, Peking University, Beijing 100871, China)

Received January 11, 2005; revised February 24, 2005

Abstract The Yalashangbo dome, located at the eastern end of North Himalayan domes zone, has a geometry and structure similar to those of a metamorphic core complex. Ductile shear zones formed the detachment system around the dome and these zones are composed of garnet-bearing phyllonite, mylonitic schist, mylonitic gneiss and mylonitic granite. Ductile shear fabrics developed well in mylonitic rocks, and penetrative lineation and foliation were formed by stretched quartz and feldspar and preferred orientation of mica. Polar Mohr diagram method is used to calculate the kinematic vorticity numbers of the shear zones in the detachment system. Results indicate that the shear zone is a thinned shear zone (thinning of 23%) in an extensional setting which underwent a general shear dominated by simple shear. Comparison of the vorticity numbers between the northern and southern flanks of the Yalashangbo dome shows that the dome is an asymmetric system formed by a north-northwest-directed detaching unanimously. Statistical fractal analysis shows that the shapes of dynamically recrystallized quartz grains in the mylonites have characteristics of self-similarity, with fractal numbers ranging from 1.05 to 1.18. From these fractal numbers, the strain rate of the rock was deduced from $10^{-9.2}\,S^{-1}$ to $10^{-7.3}\,S^{-1}$, the differential paleao-stress was 13.7—25.6 MPa during the deformation happened at a temperature over 500 ℃. The ductile shear zones in the detachment system around Yalashangbo dome were formed under a high green-schist grade condition or happened simultaneously with the intrusion of granite.

Keywords: Yalashangbo dome, ductile shear zone, kinematic vorticity, fractal analysis, deformation temperature, strain rate.

Himalaya is the young orogen formed by the India-Asia collision, but its extensional structures began to be an important component in this orogenic belt since Miocene[1]. These extensional structures include the southern Tibetan detachment system (STDS)[2,3], and the north-south striking rifts[4—8]. In addition, another kind of extensional structure has been found in north Himalaya which formed the North Himalayan domes zone (or north Himalayan antiform)[9—12]. This zone is located in southern Tibet between the STDS in south and Yarlung Zangbo suture in north (Fig. 1). In this zone, a series of isolated gneiss or granite domes exposed in Tethyan Himalaya[9—12]. Most domes are cored by two-mica granite or leucogranite plutons with cooling ages of 9.5—17.6 Ma[9, 13—15]. The core plutons are structurally mantled by mylonitic granite and gneiss, which are in turn overlain by low-grade Tibetan sedimentary rocks of Paleozoic-Mesozoic time[9, 13, 14, 16].

Yalashangbo dome is a typical doming structure in the North Himalayan domes zone and it has a similarity in structural patterns to a metamorphic core complex (Fig. 2). The main detachment fault separating the dome's gneisses and the overlying sedimentary rocks may be an exposure of the STDS. Therefore, this dome was possibly formed by the north-directed detachment of STDS[1)]. To assess some rheological and kinematic parameters using polar Mohr diagram and fractal analysis, our study focuses on the ductile shear zone around the dome. These parameters provide quantitative and qualitative evidence for the study on the forming mechanism and classification of domes and metamorphic core complexes.

1 Geology of Yalashangbo dome

Yalashangbo dome is located in the easternmost end of the North Himalayan domes zone (Fig. 1). Its geographic location is at 90°45′E—92°20′E and 28°35′N—28°55′N, and has a coverage of about 1000 km^2 (Fig. 2). The core of this circular-shape dome is composed of a leucogranite pluton and High Himalayan crystal rocks including gneiss, gneissic

* Supported by the Special Project for Authors of the National Best Ph. D Dissertations in College and University (Grant No. 200022), and the National Natural Science Foundation of China (Grant Nos. 40172074 and 49802020)

** To whom correspondence should be addressed. E-mail: pkuzhangbo@sina.com

1) Zhang J. and Guo L. Yalashangbo dome: a metamorphic core complex and the exposure of Southern Tibetan Detachment System in northern Himalaya (unpublished).

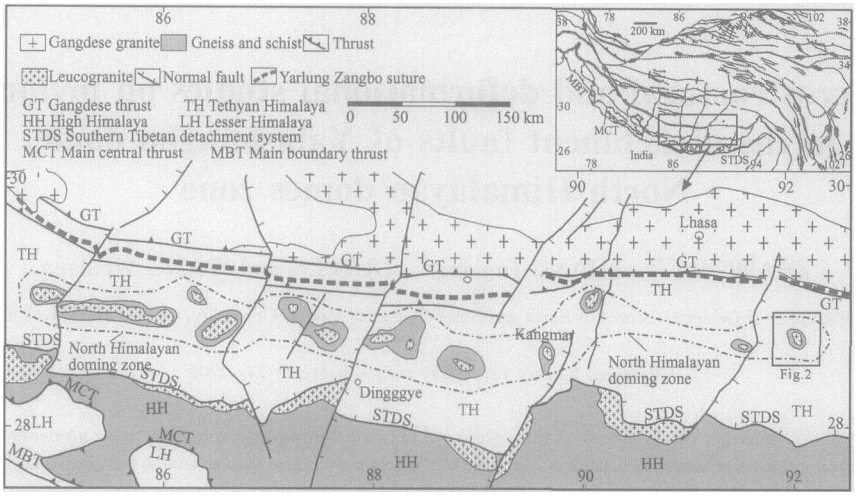

Fig. 1. Regional geological map of the North Himalayan domes zone[1)].

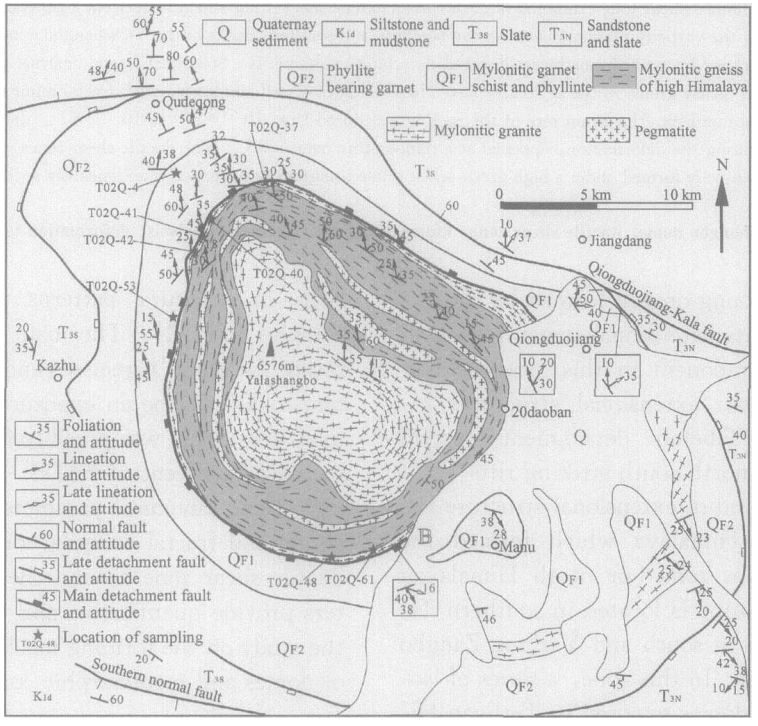

Fig. 2. Structural map of Yalashangbo dome[1)].

granite and amphibolite. Mylonitic fabrics developed very well in these crystal rocks. For example, stretched quartz, feldspar grains and alignment of mica formed the penetrative lineation and foliation, which indicates that these rocks experienced strong ductile shearing. The core pluton of dome has a cooling age of about 13 Ma (unpublished data) and an exposure of 140 km^2. The flow structures in the pluton are parallel to the ductile fabrics in the country rocks. The low-grade and weak-deformed Tibetan sedimentary sequence makes up the upper plate of the Yalashangbo dome. These low-grade rocks include slate, schist, and phyllite. Gabbro-diabase intrusions emplaced along the beddings or foliation of the low grade rocks, and they underwent deformation and metamorphism similar to their country rocks. A detachment system separated the dome core and the upper plate. It developed around the core of the dome and shaped the geometry of the dome. The detachment system may be an exposure of the STDS that

1) See the footnote on page 1005

separated the High Himalaya crystal rocks from the low-grade covering sedimentary sequence[1)].

2 Ductile deformational characteristics of mylonite zones

Mylonite zones, surrounding the Yalashangbo dome, formed the outer shell. These zones are mainly composed of garnet phyllonite, mylonitic gneiss and schist, mylonitic granite, and leucogranites with flow structures.

Mylonitic foliation, stretching and preferred oriented mineral lineations are the chief penetrative structures in rocks of the shear zones. Various foliations occurred in different rocks in the dome. They were formed by preferred orientation of quartz, plagioclase and mica grains in leucogranites pluton coring the dome, while they are represented by the thin compositional layers and intensive stretching of minerals in the high Himalyan mylonitic gneisses. Foliations in mylonitic schist and phyllite are made up of intensively stretched fine-grained matrix; they are generally planar except some bending around grains of garnet. In mylonite granite with penetrative foliations, coarse feldspar grains formed typical σ-type perphyroclastic systems. Their long axes aligned along the S foliation while their tails oriented to the C foliation together with the quartz ribbons and mica grains. These two foliations formed the S-C fabrics. In gneisses of high Himalaya, alternative layers of recrystalized feldspar, quartz ribbons and micas striped gneisses were developed. The thickness of compositional strip varies from 1 mm to 5 mm. These layers are parallel to each other and form the shear foliations of these rocks.

Penetrative mineral lineations represent the movement at an early stage of deformation along the main detachment faults, which is indicated by asymmetric perphyroclasts, and the S-C fabrics is a north-norhtwestward detachment (Fig. 2). Besides these early lineations with north-northwest and south-southeast plunges, some later lineations developed on some later brittle-ductile foliations in the dome, such as hot striae and mineral fibers. They display down-dip plunges along the foliations toward the outsides of the dome. These lineations likely resulted from a "diapirism process" at a later stage. This "diapirism" drove the core of the dome uplifting further and finally caused the collapse of the dome, which is represented by the later down-dip lineations on brittle-ductile foliations.

Abundant micro-structures with extensional features were preserved in mylonitic zone of the main detachment faults, such as domino structure, core-mantle structure, σ-type porphyroclastic system, mica-fish structure, etc. In core-mantle structures, the cores were mainly elongated and asymmetric feldspar grains. The surrounding mantles were dynamically recrystalized feldspar and quartz grains with diameters between 20 μm and 250 μm. Porphyroblasts grew penetratively in the rocks, and they are chiefly garnet, plagioclase and microcline. The grain-sizes of the porphyroblasts vary greatly and their diameters range from 1—2 mm to 30 mm. Some Porphyroblasts contain inclusions of quartz, biotite, and sillimanite, and these inclusions have a shape-preferred orientation which is oblique to C-foliation in matrix. A lot of core-mantle structures are cored by quartz grains with zigzag boundaries, which are mantled by fine-grained recrystallized quartz. The fine quartz grains in mantles have a shape-preferred orientation. Dynamic recrystallization in quartz grains (Fig. 3) are the most popular micro-structures in the shear zone. Their irregular boundaries possibly indicate a static plastic flow under high-temperature and low stress rate.

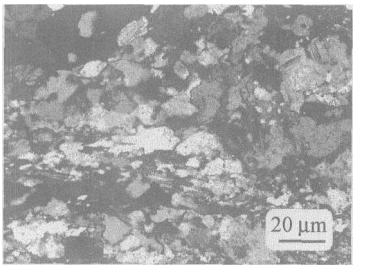

Fig. 3. Dynamically recrystallized quartz grains with irregular grain boundaries.

3 Kinematic vorticity number and shear type of the Yalashangbo dome

It is one of the important issues to understand the formation mechanisms of a metamorphic core complex. A number of approaches have been proposed, among which, determination of the kinematic vorticity number and the shear type of a metamorphic core complex is recognized as one of the most efficacious and direct ways. Shear zones in nature were developed in co-actions of pure and simple shearing, and named general shear zones. To some extent, kinematic vorticity number (ω_k) appears to be an ideal parameter to characterize the ratio of pure shearing to

1) See the footnote on page 1005

simple shearing in a general shear zone. Among the methods of detecting kinematic vorticity number in rocks[17—25], polar Mohr diagram is regarded as one of the most simple and practical tools[20—22]. In this paper, polar Mohr diagram method is used for determining the kinematic vorticity of the shear zones in Yalashangbo dome.

Polar Mohr diagram was proposed firstly by Simpson and De Paor[26]. Once a polar Mohr diagram is constructed, Kinematic vorticity number (ω_k) and relations between ω_k, ν and ε/γ (ε and γ are strain-rate of pure and simple shear, respectively) can be calculated by $\omega_k = \cos(\nu)$, where ν is the angle between the two eigenvectors on the XZ plane in a shear zone. One of the three practical methods devised by Zhang and Zheng[20—22], i.e. construction of a polar Mohr circle with R_s (axial ratio of a strain ellipse) and α (angles between the long axes of strain ellipse and shear foliation) (Fig.4) is used here.

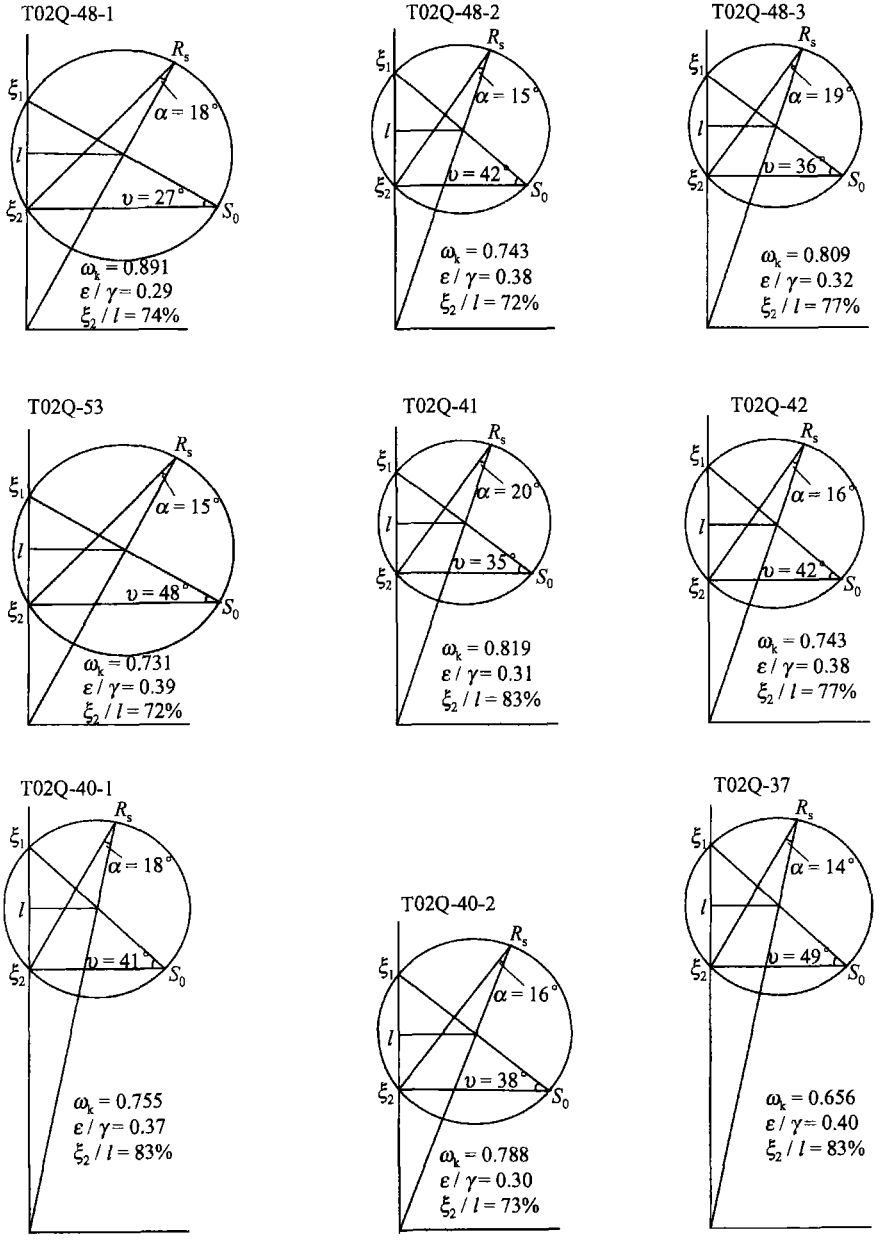

Fig. 4. Polar Mohr diagrams in mylonitic zone of the detachment faults. α, angle between the long axe of a strain ellipse and the shear foliation; R_s, axial ratios of the strain ellipse; ξ_1 and ξ_2, two eigenvectors; S_0, anchor point; ν, angle between the two eigenvectors; ω_k, kinematic vorticity number; ε/γ, ratio of pure shear strain rate to simple shear rate in the shear zone; ξ_2/l, change in thickness of a shear zone (the ratio of the present thickness to the original thickness of the shear zone).

Kinematic vorticity numbers of the mylonitic zone in Yalashangbo dome are measured and calculated with the technique of polar Mohr construction. The sites of sampling are shown in Fig. 2, and results are listed in Table 1. The angles between the two eigenvectors in the mylonitic zone range between 27° and 49°, corresponding to kinematic vorticity numbers from 0.656 to 0.891.

Few natural shear zones have developed into pure shear zones or simple shear zones, and usually, most of them are general shear zones. Because there is a wide range of general shear type, determining the ratio of pure shear component to simple shear component is essential to identify the shearing type in a shear zone. According to the kinematic vorticity theory, $\nu = 90°$, $\omega_k = 0$ stands for coaxial pure shear; $\nu = 0°$, $\omega_k = 1$ represents simple shear; and $0° < \nu < 90°$, $0 < \omega_k < 1$ corresponds to general shear[26]. The kinematic vorticity numbers (ω_k) of the shear zone within Yalashangbo dome range between 0 and 1, which indicates a general shearing type, i.e. combination of pure shear and simple shear components with different ratios. The relative positions of $(\xi_1, 0)$ to $(\xi_2, 0)$ in polar Mohr diagrams can be used to deduce the shearing character and the changes in thickness of the shear zone[21—23]. Within Yalashangbo shear zone, $\xi_1 > \xi_2$ reveals that the shear zone was thinned to be about 23% of the original thickness (Table1). $\varepsilon/\gamma = 0.29$—$0.40$ implies a simple-shear dominating shearing. In one word, the shear zone in Yalashangbo dome is a simple-shear dominating and thinned general shear zone. In addition, the average kinematic vorticity number (ω_k) is about 0.814 in southern flank of the dome, while it is about 0.735 in the northwest flank, which means more simple-shear component involved in the southern part of the dome. Therefore, the Yalashangbo dome may be an extensional structure formed by an active northwestward detachment fault, similar to a metamorphic core complex.

Table 1. Rheology parameters of the detachment faults within the Yalashangbo dome

Location of sampling	Polar Mohr circle method $\omega_k = \cos\nu$						Other parameters	
	Thin section	Numbers	R_s	α	ν	ω_k	Change of thickness: ξ_2/l	Ratio of strain rates: ε/γ
Main detachment fault, southern flank of the dome	T02Q-48-1	50	3.20	18	27	0.891	74%	0.29
	T02Q-48-2	20	2.31	15	42	0.743	72%	0.38
	T02Q-48-3	30	2.19	19	36	0.809	77%	0.32
Main detachment fault, southwestern flank	T02Q-53	45	2.24	15	43	0.731	72%	0.39
Main detachment faults, northwestern flank	T02Q-41	50	2.11	20	35	0.819	83%	0.31
	T02Q-42	30	2.06	16	42	0.743	77%	0.38
The northern main detachment faults of the dome	T02Q-40-1	50	1.64	18	41	0.755	83%	0.37
	T02Q-40-2	35	2.46	16	38	0.788	73%	0.30
	T02Q-37	40	1.55	14	49	0.656	83%	0.40

4 Estimation of deformation temperature and strain rate for the ductile shear zone

One of the key issues in studying ductile shear zones is to assess the temperature and strain rate during the shearing deformation, because deformation mechanisms of rocks and minerals are affected by these two factors. Based on the studies of microstructure and experimental structure, Kruhl and Nega introduced a new method for calculating the deformation temperature and strain rate[27,28]. They developed this technique from the geometrical boundaries of dynamically recrystallized quartz grains that had characteristics of fractal dimension, and the fractal dimension could be used as geothermometer and strain rate meter. They established a diagram of the relation between the deformation temperature and the fractal dimensions of dynamically recrystallized quartz grains (Fig. 5).

Experimental studies show that the fractal dimension systematically increases with increasing strain rate at a constant temperature, while it decreases with increasing temperature under a constant strain rate. The fractal dimension is interpreted to be an indicator for some deformation conditions due to its systematical change under these deformational conditions. The theoretical relation between the fractal dimension (D), deformation temperature T(K) and strain rate ε (s^{-1}) was suggested by Takahashi et al.[29], which can be expressed as a least-squares fitted equation:

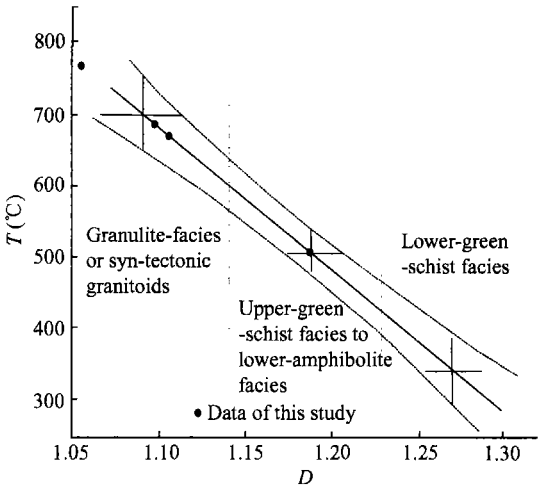

Fig. 5. Diagram showing the relation between fractal dimensions and deformation temperature[28].

$$D = \phi \log\varepsilon + \rho/T + 1.08, \quad (1)$$

where $\phi = 9.34 \times 10^{-2}\{[\log(s^{-1})]^{-1}\}$, and $\rho = 6.44 \times 10^{2}(K)$.

Although dynamically recrystallized quartz crystals are sensitive to post-deformation recovery, which can disturb the reliability of results estimated by the method, practical and experimental studies have shown that this new method is, to a certain extent, effective and practicable to assess the deformational temperature and strain rate[29,30].

4.1 Estimation of deformation temperature

Fractal dimensions of dynamically recrystallized quartz grains are calculated from photographs of six thin sections from Yalashangbo shear zone. There are two microstructural characteristics for these dynamically recrystallized new quartz crystals: (1) irregular grain boundaries such as elongated and zigzag; (2) weak preferred orientation of the grains. These characteristics of the quartz grains in granitic mylonites make it convenient for determining the deformation temperature using fractal dimension.

Two methods are suitable for determining the fractal dimension (D) from recrystallized quartz grain boundaries: one is the closed-zigzag-line method and the other is the area-perimeter method[30]. In this paper, area-perimeter method is used. The approach is as follows: Firstly, dynamically recrystallized grains on each thin section are photographed with scale. Secondly, the boundary of each grain is traced on the photo by software MapInfo 7.0. Thirdly, the actual perimeter P and area A of this traced quartz grain are determined by the intellectualized software. Fourthly, the diameter d of a circle with a same area A is calculated. The perimeter P and diameter d of all quartz grains in the photographs of the thin sections are measured and calculated through the above steps. Fifthly, plot P and d in a coordinate frame using Excel, with (Log P) as the vertical axis and (Log d) as the horizontal axis, respectively. Finally, the fractal dimension D is defined as the slope of the least-squares fitted line for the plots. The results of fractal dimension of analyzed samples and the plots of log$P$ versus log$d$ are shown in Table 2 and Fig. 6.

The correlation coefficients for statistics of quartz grain boundaries are more than 0.8 for all the six samples. Numbers of fractal dimension are 1.04 and 1.01, respectively, in the two samples from the hanging-wall of the main detachment faults of Yalashangbo dome. Number of fractal dimension ranges from 1.05 to 1.18 in the samples from main detachment faults. Thus, shapes of dynamically recrystallized quartz grains in mylonites are statistically self-similar ($1 \leqslant D \leqslant 2$), and the fractal dimension can imply deformation temperature[27,28]. According to Kirul et al.'s geometric temperature gauge (Fig. 5), the shear zone mantling the Yalashangbo dome underwent a deformation at a temperature not lower than 500 ℃. This means that deformation possibly occurred at a temperature higher than that for high greenschist facies, or the leucogranite intruded during deformation.

The above results have been proved by microscopical and field investigation. Under a microscope, ribbons of hornblende and fine-grained plagioclase are observed with zonations. Amphibolites were metamorphosed from mafic rocks with mineral assemblage of hornblende + plagioclase + biotite + quartz + epidote + garnet. Further enlarged micro-images reveal new growing and fine grains of pyroxenes and feldspars that developed between hornblendes and feldspars in metamorphosed and deformed mafic rocks. Additionally, plastically elongated feldspar and ribbons of quartz (axial ratio > 10) were well-developed. All micro- characteristics can be attributed to high-temperature deformation. Macroscopically, gneiss xenoliths in granitic mylonite had been assimilated completely and were stretched strongly along stretching lineation. Meanwhile, granite has some characteristics of syn-tectonic emplacement[1)].

1) See the footnote on page 1005

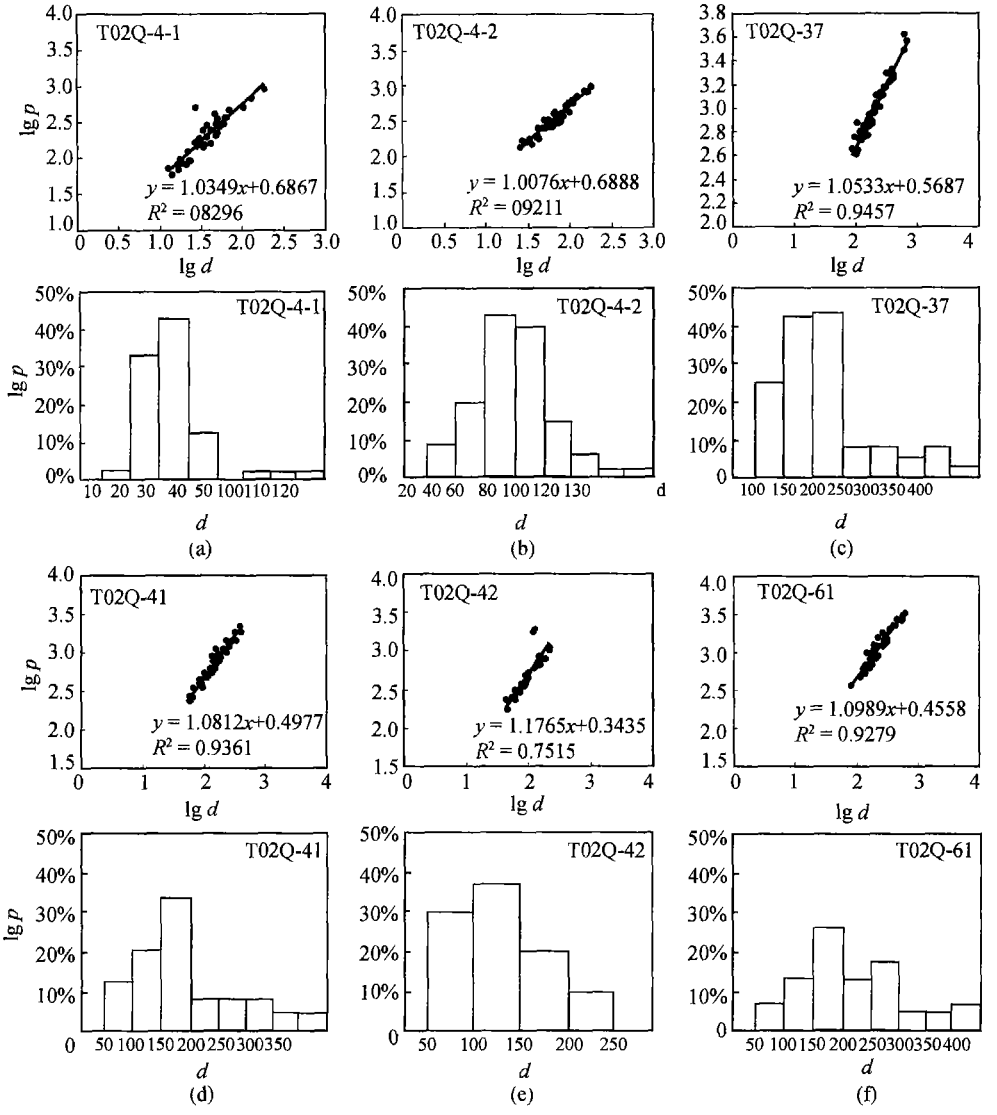

Fig. 6. Diagrams of coordinate plots of Log P versus Log d, and histograms below the coordinate plots showing the frequencies against d. P, perimeter of the dynamically recrystallized quartz grain; d, diameter of the circle with a same area to the measured grain; y ($y = 1.176x + 0.34$), the least-square fitted linear equation, the fractal dimension of 1.176 is given by the slope of the equation; f, the frequency of grain diameters; R^2, the correlation coefficient.

Table 2. Fractal characteristics of dynamically recrystallized quartz grains of mylonites in ductile shear zone of Yalashangbo dome

Location of samples	Sample No.	Statistical numbers	Grain diameter μm	Mean diameter μm	Grain perimeter μm	Fractal dimension	Correlation coefficient	Strain rate S^{-1}	Different stress MPa
Hanging-wall	T02Q-4-1	39	12.8—183.6	42.1	71.3—913.1	1.03	0.83	$10^{-8.9}$	48.0
	T02Q-4-2	48	25.7—185.1	72.0	133.8—955.6	1.01	0.92	$10^{-9.2}$	33.3
Main detachment fault	T02Q-37	57	84.7—619.5	216.0	413.4—3750.5	1.05	0.95	$10^{-8.7}$	15.8
	T02Q-41	39	57.4—416.2	165.2	245.1—2232.2	1.08	0.94	$10^{-8.4}$	18.9
	T02Q-42	29	45.0—220.9	106.7	44.6—1741.9	1.18	0.75	$10^{-7.3}$	25.6
	T02Q-61	46	81.8—581.9	263.8	364.4—3269.9	1.09	0.93	$10^{-8.3}$	13.7

4.2 Estimation of strain rates and paleo-stress

If the deformation temperature was 550 ℃ during shearing, the strain rate can vary in the range from $10^{-9.2}$ S^{-1} to $10^{-7.3}$ S^{-1} according to Eq. (1) proposed by Takahashi et al.[29]. This is a mid-high strain rate. Wang et al. applied this fractal dimension method to ductile shear zones of the late Archean time

in western Shandong. They deduced a range of paleo-strain rates from $10^{-7.6}$ s^{-1} to $10^{-8.7}$ s^{-1}, also falling in the range of mid-high strain rate[30]. However, natural geological strain rates are estimated to lie usually between 10^{-13} s^{-1} and 10^{-15} s^{-1}[31,32]. Further study is needed for the difference between geological strain rates and experimental statistic ones.

As shown in Table 2, diameters of dynamically recrystallized quartz grains are in the range of 42.0—263.8 μm. From these data and according to the palaeopiezometer of Twiss[33] ($\Delta\sigma = 610 \times d^{-0.68}$), differential palaeo-stress is estimated to be from 13.7 MPa to 25.6 MPa in the mylonites from the main detachment fault of the Yalashangbo dome.

5 Discussion and conclusion

(1) Macro and micro ductile deformational fabrics were formed penetratively in the deformed rocks in the mylonitic zones mantling the Yalashangbo dome. The macro-fabrics include mylonitic foliation, lineation and S-C, etc. The microstructures have typical characteristics of ductile deformation and shear sense, such as mica-fish, kink structure of mica, core-mantle structure, and rotationed porphyroclastic system. All the micro and macro indicators show consistently a north-northwest-directed detachment movement in the main detachment faults.

(2) Two-dimensional kinematic vorticity numbers of the main detachment faults in Yalashangbo dome were systemically measured using polar Mohr construction. The kinematic vorticity numbers related to the shear zone range from 0.656 to 0.891, which represents a general shear. $\varepsilon/\gamma = 0.29$—$0.40$ indicates a simple-shear dominating the general shear zone. $\xi_1 > \xi_2$ means the shear zone was thinned. The average ratio of the present thickness to the original thickness of the shear zone is about 77% (ξ_2/l). Numbers of kinematic vorticity (ω_k) in southern flank of the Yalashangbo dome are higher than those in northwestern flank, which shows a more simple-shearing component involved in the southern shear zone. Therefore, the Yalashangbo dome is an asymmetry extensional system formed by active northwestward detachment.

(3) Typical dynamically recrystallized quartz grains developed extensively in mylonites of the main detachment faults of the Yalashangbo dome. This provides good condition for fractal dimension analysis, and the analytical results show that: Shapes of these new crystals have characteristics of statistical self-similarity, and their fractal dimension ranges from 1.01 to 1.18. Paleo-strain rates and palaeo-stress were initially estimated to be $10^{-9.2}$—$10^{-7.3}$ S^{-1} and 13.7—25.6 MPa, respectively. Deformation temperature of the shear zone of the dome was calculated to be higher than 500 ℃. This presents that the deformation possibly occurred at a high temperature or during the emplacement of the leucogranite.

References

1 Yin A. and Harrison T. M. Geologic evolution of the Himalayan-Tibetan orogen. Annu. Rev. Earth Planet. Sci., 2000, 28: 211—280.

2 Burg J. P., Brunel M., Gapais D. et al. Deformation of the crystalline main central sheet in south Tibet (China). J. Struct. Geol., 1984, 6: 535—542.

3 Burchfiel B. C., Chen Z., Hodges K. V. et al. The south Tibetan detachment system, Himalayan orogen, extension contemporaneous with and parallel to shortening in a collisional mountain belt. Geol. Soc. Am. Special Paper 269, 1992, 1—41.

4 Coleman M. and Hodges K. Evidence for Tibetan plateau uplift before 14 Myr age from a new minimum age for east-west extension. Nature, 1995, 374: 49—52.

5 Harrison T. M., Copeland P., Kidd W. S. F. et al. Activation of the Nyainqentanghla Shear Zone: Implication uplift of the southern Tibetan Plateau. Tectonics, 1995, 14: 658—676.

6 Yin A. Mode of Cenozoic east-west extension in Tibet suggesting a common origin of rifts in Asia during the Indo-Asian collision. J. Geophys. Res., 2000, 105(B9): 21745—21759.

7 Zhang J., Ding L., Zhong D. et al. Orogen-parallel extension in Himalaya, Is it the indicator of collapse or the product in process of compressive uplift? Chinese Science Bulletin, 2000, 45: 114—119.

8 Zhang J., Guo L. and Ding L. Structural characteristics of middle and southern Xainza-Dinggye Normal Fault System and its relationship to Southern Tibetan Detachment System. Chinese Science Bulletin, 2002, 47: 1063—1069.

9 Burg J. P., Guiraud M., Chen G. M. et al. Himalayan metamorphism and deformation in the North Himalayan belt, southern Tibet, China. Earth Planet. Sci. Letts., 1984, 69: 391—400.

10 Chen Z., Liu Y., Hodges K. V. et al. The Kangmar Dome: a metamorphic core complex in southern Xizang (Tibet). Science, 1990, 250: 1552—1556.

11 Lee J., Dinklage W. S., Hacker B. R. et al. Evolution of the Kangmar Dome, southern Tibet: structure, petrologic, and thermochronologic constraints. Tectonics, 2000, 19: 872—892.

12 Lee J., Hocker B. and Wang Y. Evolution of North Himalayan gneiss domes: structural and metamorphic studies in Mabja Dome, southern Tibet. J. Struct. Geol., 2004, 26: 2297—2316.

13 Debon F., Le Fort P., Sheppard S. M. F. et al. The four plutonic belts of the Transhimalaya-Himalaya: a chemical, mineralogical, isotopic, and chronological synthesis along a Tibet-Nepal section. J. Petrol., 1986, 27: 219—250.

14 Schärer U., Xu R. and Allegre C. U-(Th)-Pb systematics and ages of Himalayan leucogranites, southern Tibet. Earth. Planet. Sci. Lett., 1986, 77: 35—48.

15 Harrison T. M., Lovera O. M. and Grove M. New insights into the origin of two contrasting Himalayan granite belts. Geology, 1997, 25: 899—902.
16 Baldwin J. A., Hodges K. V., Bowring S. A. et al. Continental subduction in the western Himalayan orogen? Geol. Soc. Am. Abstracts with Programs, 1998, 30: 269—282.
17 Passchier C. W. Stable position of rigid objects in non-coaxial flow-a study in vorticity analysis. J. Struct. Geol., 1987b, 9: 679—690.
18 Weijermars R. Talor-mill analogues for patterns of flow and deformation in rocks. J. Struct. Geol., 1998, 20: 77—92.
19 Beam E. C. and Fisher D. M. An estimate of kinematic vorticity from rotated elongate porphyroblasts. J. Struct. Geol., 1999, 21: 1553—1559.
20 Zhang J. and Zheng Y. Polar Mohr constructions for strain analysis in general shear zones. J. Struct. Geol., 1997, 19(5): 745—748.
21 Zhang J. and Zheng Y. Kinematic vorticity, polar Mohr circle and their application in quantitative analysis of general shear zones. J. Geomechanics (in Chinese), 1995, 1(3): 55—64.
22 Zhang J. and Zheng Y. Basic principles and applications of kinematic vorticity and polar Mohr diagram. Geological Science and Technology Information (in Chinese), 1997, 3(16): 33—39.
23 Bobyarchick A. R. The eigenvalues of steady state flow in Mohr space, Tectonophysics, 1986, 122: 35—51.
24 Weijermars R. The role of stress in ductile deformation. J. Struct. Geol., 1991, 13(9): 1061—1078.
25 Weijermars R. Taylor-mill analogues for patterns of flow and deformation in rocks. J. Struct. Geol., 1998, 20: 77—92.
26 Simpson C. and De Paor D. G. Strain and kinematic analysis in general shear zones. J. Struct. Geol., 1993, 15: 1—20.
27 Kruhl J. H., Nega M. and Milla H. E. The fractal shape of grain boundary sutures: reality, model and application as a geothermometer. In: 2nd Int. Conf. on Fractal and Dynamic Systems in Geosciences. Frankfurt, Book of Abstracts, 1995, 84: 31—32.
28 Kruhl J. H. and Nega M. The fractal shape of sutured quartz grain boundaries: application as a geothemometer. Geologishe Rundschau, 1996, 85: 38—43.
29 Takahashi M., Nagahama H. and Masuda T. Fractal analysis of experimentally, dynamically recrystallized quartz grains and its possible application as a strain rate meter. J. struct. Geol., 1998, 20(2/3): 269—275.
30 Wang X.S., Zheng Y., Yang C. et al. Determination of the deformation temperature and strain rate by the fractal shape of dynamically recrystallized quartz grains. ACTA Petrol. ET Mineralogica (in Chinese), 2001, 20(1): 36—41.
31 Pfiffner O. and Ramsay J. Constraints on geological strain rates-arguments from finite strain states of naturally deformed rocks. J. Geophys. Research, 1982, 87: 311—321.
32 Carter N. and Tsenn M. Flow properties of continental lithosphere. Tectonophysics. 1987, 136: 27—63.
33 Twiss R. J. Theory and applications of a recrystallized grain size paleopiezimeter. Pure Appl. Geophys., 1977, 115: 227—244.